Biochimica et Biophysica Acta 1853 (2015) 604–610

Contents lists available at ScienceDirect

Biochimica et Biophysica Acta

journal homepage: www.elsevier.com/locate/bbamcr

Monitoring of autophagy is complicated—salinomycin as an example

Jaganmohan Reddy Jangamreddy [a], Soumya Panigrahi [b], Marek J. Łos [a,c,*]

[a] Department of Clinical and Experimental Medicine (IKE), Division of Cell Biology and Integrative Regenerative Medicine Center (IGEN), Linköping University, Sweden
[b] Department of Medicine/Infectious Diseases, Case Western Reserve University, Cleveland, OH 44106, USA
[c] Department of Pathology, Pomeranian Medical University, Szczecin, Poland

ARTICLE INFO

Article history:
Received 4 November 2014
Received in revised form 10 December 2014
Accepted 11 December 2014
Available online 23 December 2014

Keywords:
Autophagic flux
GFP-LC3
mTandem GFP-RFP LC3
p62/SQSTRM1
Vacuolization
Salinomycin

ABSTRACT

Monitoring of autophagy is challenging because of its multiple steps and lack of single befitting technique for a complete mechanistic understanding, which makes the task complicated. Here, we evaluate the functionality of autophagy triggered by salinomycin (anti-cancer stem cell agent) using flow cytometry and advanced microscopy. We show that salinomycin does induce functional autophagy at lower concentrations and such a dose is cell type-dependent. For example, PC3 cells show active autophagic flux at 10 μM concentration of salinomycin while murine embryonic fibroblasts already show an inhibition of flux at such doses. A higher concentration of salinomycin (i.e. 30 μM) inhibits autophagic flux in both cell types. The data confirms our previous findings that salinomycin is an inducer of autophagy, whereas autophagic flux inhibition is a secondary response.

1. Introduction

Autophagy is the primary cellular metabolic stress-induced catabolic response that converts organelles, pathogens and cellular debris to its building blocks that are eventually recycled. A dysfunctional autophagy promotes carcinogenesis, while a functional autophagy is necessary for cancer cell survival under extreme conditions of hypoxia and nutrient deprivation [1]. Thus, the definition of chemotherapeutic agents in their role as either inducers or inhibitors of functional autophagy is pivotal for proper planning of treatment. The complexity of autophagic process and the lack of one robust standard technique to follow its progression warrant the employment of several techniques. Standardization of techniques to precisely monitor autophagy is constantly evolving [2].

Macroautophagy, referred to in this article as autophagy, triggered either by activation of class III PI3-kinases or inhibition of class I PI3-kinases, initiates the formation of an initial phagophore that matures to a double-membraned envelope, which engulfs the substrates. The engulfed material is then degraded upon fusion with acidic lysosomes. The initiation of autophagy is a tightly regulated sequential process governed by multiprotein complexes composed of autophagy-related proteins. To name a few examples in sequential order during autophagy initiation: Beclin1, ATG5, ATG7 and LC3 (ATG8) along with other cellular proteins, those that are degraded by autophagy like p62/SQSTRM1 are traced to identify functional autophagy. Beclin1 marks the initiation of autophagy, and forms a complex with autophagy initiation multimer involving UVRAG and UMBRA [3]. This initiation is followed by the elongation of the phagophore through ATG5- and ATG7-dependent mechanisms leading to the lipidation of LC3 to form LC3II and consequent recruitment to the elongating phagophore [3]. Thus, mitigation of LC3II acts as a major tool to evaluate the elongation of the phagophore. LC3II is localized on either side of the membrane. Upon maturation of the autophagosome by fusing with lysosomes, part of LC3II localized to the inner membrane gets degraded while the rest on the outer membrane is recycled. Hence, monitoring of LC3 is widely used as it acts not only as a marker for autophagy induction but also to study maturation of the autophagosome. More notably, autophagy monitoring studies using tagged LC3 with either GFP (green florescent protein) alone, or with tandem GFP and RFP (red florescent proteins), or most recently, Wasabi as a replacement for GFP has become the standard [4]. Since lysosomes ultimately define the active, functional autophagy, staining of these acidic organelles, to determine the number of lysosomes and their localization to autophagosomes (their fusion marks the completion of autophagic process), are also frequently used for monitoring autophagy.

Streptomyces albus–derived ionophore salinomycin (Sal) is widely studied because of its potency to kill cancer stem–like cells [5,6]. We, along with other groups, have shown that salinomycin's toxicity towards cancer and cancer stem cells depends on the disruption of function of mitochondria [6,7]. We employ a wide range of breast cancer, prostate cancer and normal primary human cells to show that salinomycin toxicity is concentration-, time- and cell type–dependent with least toxicity towards normal primary fibroblasts [6]. However, there are conflicting

* Corresponding author at: Department of Clinical and Experimental Medicine, Integrative Regenerative Medicine Center (IGEN), Linköping University, Cell Biology Building, Level 10, 581 85 Linköping, Sweden. Tel.: +46 10 10 32787.
E-mail address: marek.los@liu.se (M.J. Łos).

http://dx.doi.org/10.1016/j.bbamcr.2014.12.022
0167-4889/

reports regarding autophagy induction by salinomycin. We, along with Li and colleagues [8], show that salinomycin induces autophagic flux, while Yue and collaborators [9] show salinomycin as an inhibitor of functional autophagy without altering the lysosomal acidity but through an unknown mechanism of attenuating lysosomal proteases. The comparison is complicated by the fact that all the above-mentioned studies employed different cancer cellular models [6,8,9]. So, in this brief report, we evaluate autophagy induced by salinomycin employing a variety of techniques including recently developed flow cytometry techniques, and live cell imaging approaches [10–12]. We show that salinomycin-induced autophagic flux is dose-, and cell type–dependent.

2. Results

2.1. Salinomycin is an inducer of autophagy and autophagic flux

We initially identified the salinomycin function in regulating autophagic flux using normal cells (MEF) and cancer cells (PC3 and SKBR3). As a follow-up to our previous study, we assessed by Western blot the ratiometric increase of LC3II accumulation in the presence of salinomycin and chloroquine compared to either salinomycin or chlorquine alone [6]. As shown in Fig. 1A and Supplementary Fig. 1A, salinomycin-treated cells (0.1 μM and 1 μM) and chloroquine-treated cells (25 μM) showed increased accumulation of LC3II, but only cells treated with 0.1 μM Sal showed a ratiometric increase in the presence of chloroquine. Even though 1 μM Sal (Fig. 1A) and 10 μM Sal (Supplementary Fig. 1B) treated cells showed increased accumulation of LC3II in the presence of chloroquine, they did not show a significant difference compared to 1 μM Sal and 10 μM Sal treated cells alone, respectively. To remedy the possibility that inhibition of autophagy by 25 μM Cq would only be partial, we increased the concentration of chloroquine to 50 μM. In the presence of 50 μM Cq, a further increase in accumulation of LC3II occurred upon 10 μM Sal treatment as compared to Cq and 10 μM Sal-treated samples independently (Supplementary Fig. 1B).

Autophagic flux was further monitored using another autophagic marker, p62/SQSTRM1, and the results correlated with that of LC3II flux. In the presence of salinomycin at 0.1 and 1 μM concentration, p62/SQSTRM1 was directed towards proteolysis in PC3 and MEF cells. The proteolysis of p62/SQSTRM1 was resistant to Cq pretreated, inferring that salinomycin does induce functional autophagy at lower concentrations (Fig. 1A and Supplementary Fig. 1A). However, there was no increase of LC3 flux in SKBR3 cells, and p62/SQSTRM1 levels remained unaltered at 1 μM Sal regardless of the presence of chloroquine (Supplementary Fig. 1A). Thus, the dosage of salinomycin differentially affects autophagic flux among cell types.

2.2. Higher doses of salinomycin inhibits autophagic flux

Based on our observations so far we hypothesized that salinomycin could inhibit autophagic flux at higher concentrations depending on

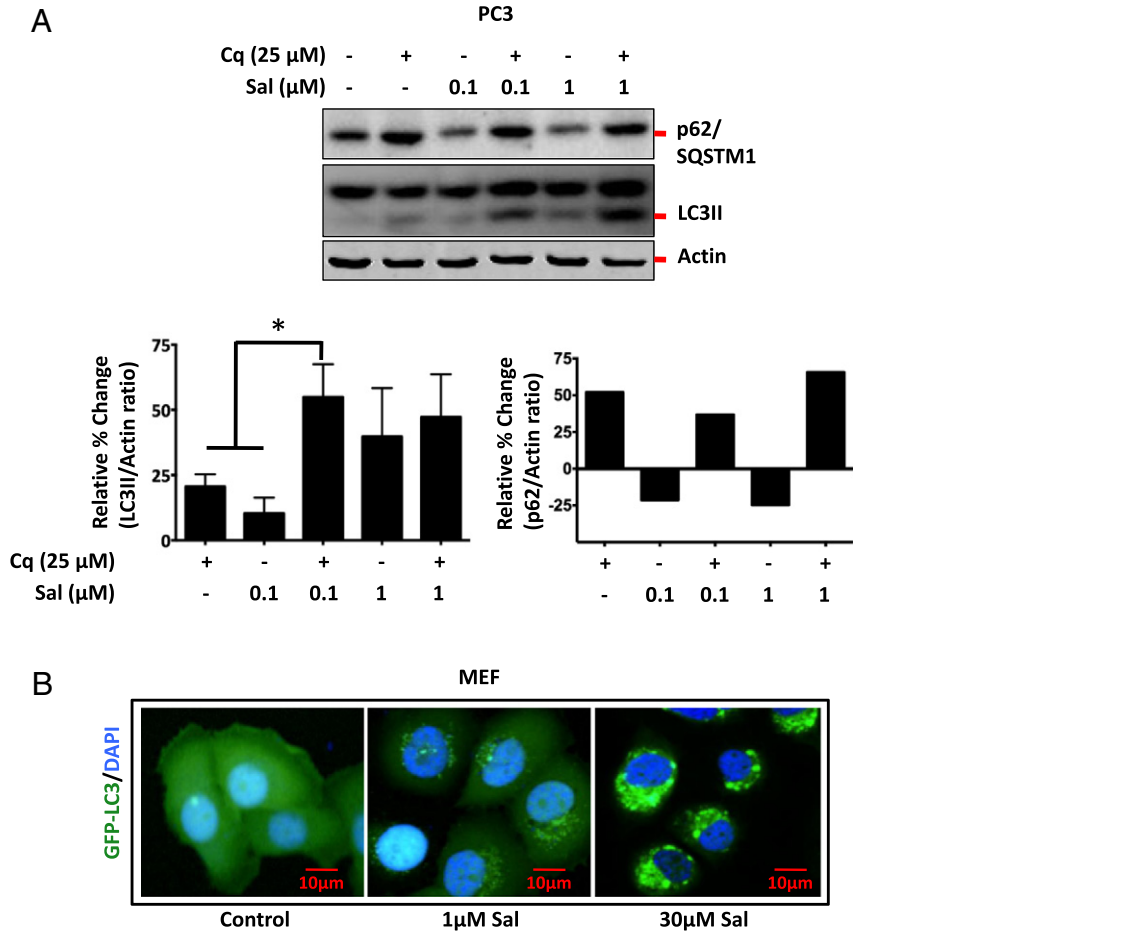

Fig. 1. Salinomycin induces autophagic flux. Autophagic flux was monitored through estimating LC3II and p62/SQSTM1 protein levels upon salinomycin treatment at different concentrations. LC3II showed increased levels upon salinomycin treatment (0.1 μM and 1 μM), but in the presence of chloroquine 0.1 μM salinomycin-treated samples showed ratiometric increase (A). Even though 1 μM salinomycin-treated samples showed increase in LC3II accumulation in the presence of chloroquine it was only a linear increase (A). p62/SQSTM1 protein levels degrade upon autophagy induction by salinomycin treatment, showing a functional autophagy and this degradation was inhibited upon chloroquine treatment (A). Confocal microscopy images of MEF cells expressing GFP-LC3 and treated with salinomycin show increased LC3 punctae (B) but 1 μM salinomycin-treated cells show distinct dots (punctae) while the 30 μM treated cells show huge vacuoles with GFP-LC3 and clumping of vacuoles near the nucleus (B). $N = 3$, $^*p < 0.05$.

cell type as different cells have different toxicity doses of salinomycin. To test this, a follow-up study with 1 μM and 30 μM salinomycin was done. As shown in Fig. 1B, GFP-LC3 expressing MEF cells treated with 1 μM salinomycin showed distinct green autophagic punctae while the control cells show homogeneous green florescence throughout the cytoplasm. Even though cells treated with higher concentrations of salinomycin showed green punctae, many cells exhibit heterogeneity in the punctae pattern as some cells show appearance of clumped GFP vacuoles while others show distinct autophagic punctae (Fig. 1B).

Following this initial observation of distinct LC3II pattern of accumulation among cells treated with different concentrations of salinomycin, we employed flow cytometric approaches to enumerate the salinomycin

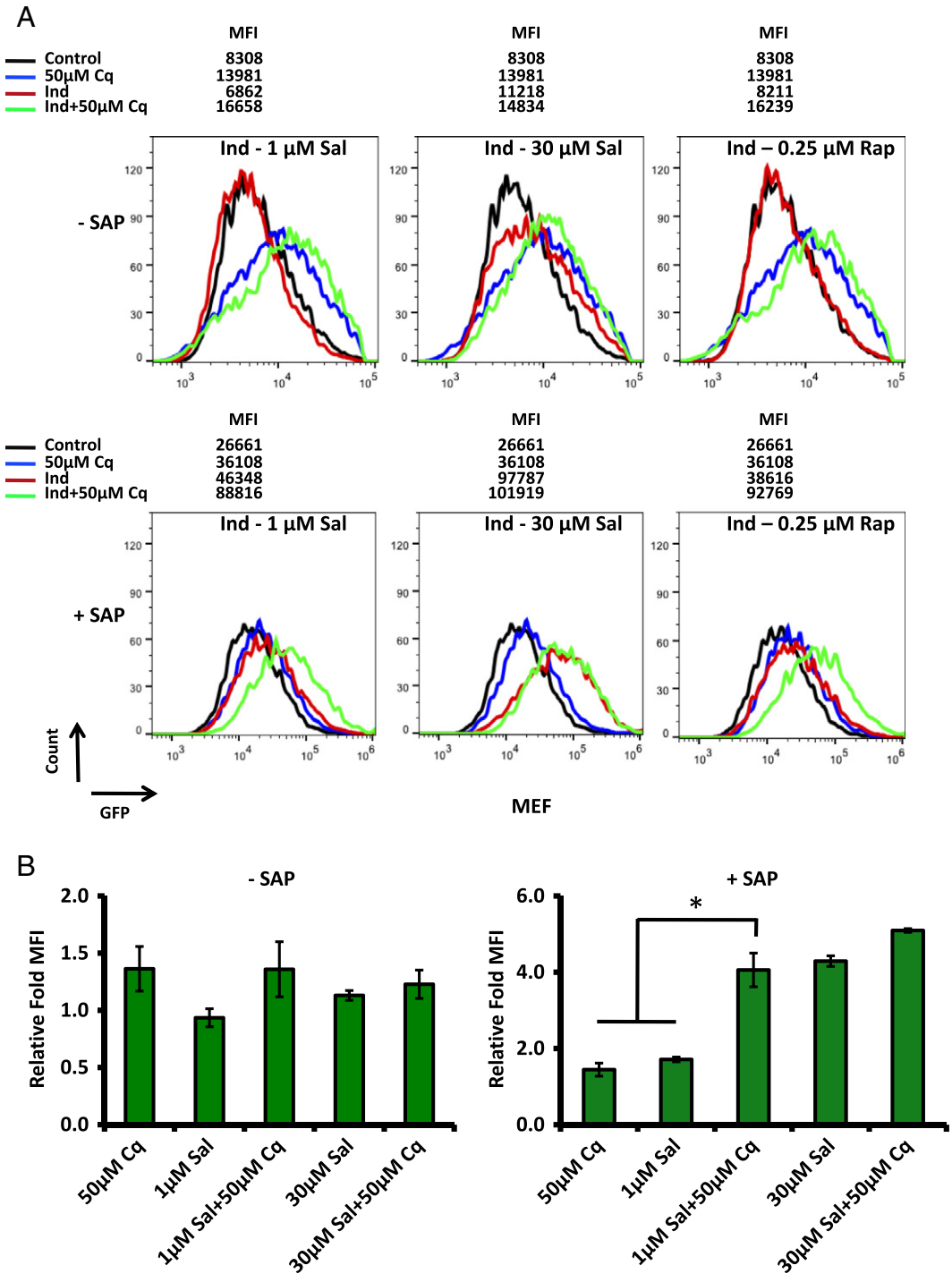

Fig. 2. Total or membrane-bound GFP-LC3 quantification for autophagic flux determination. GFP-LC3 expressing MEF cells treated with salinomycin either in the presence of autophagy inhibitor chloroquine or alone are subjected to flow cytometry to estimate the total green florescence. Treatment with 1 μM salinomycin or 0.25 μM rapamycin (positive control) show decreased median florescence intensity (MFI) of green florescence compared to control. Chloroquine treatment shows an increase in MFI due to the inhibition of autophagy either in the presence of autophagic inducer (salinomycin or rapamycin) or by itself. Samples treated with 30 μM of salinomycin show similar increase in MFI as chloroquine and thus show that salinomycin at higher concentrations inhibits autophagic flux (upper panel: A). MEF cells were treated with saponin to remove the cytoplasmic unbound GFP-LC3 to facilitate the estimation of LC3 bound to autophagic vacuoles shows increase in MFI both in the presence of inhibitors of functional autophagy (chloroquine and 30 μM Sal) as well as inducers of autophagy (1 μM Sal and 0.25 μM Rap). Chloroquine pretreated cells in the presence of 1 μM Sal and 0.25 μM Rap shows tremendous increase in MFI but not in the presence of 30 μM Sal (lower panel: A). Quantitative representation of MFI values either in the presence or absence of saponin for the above (B). $N = 4$, $^{*}p < 0.05$.

triggered autophagic flux using GFP-LC3 expressing cells as described previously by Shvets et al. and Eng et al. [10–12]. In the presence of active autophagy, GFP-LC3 that is located to the inner membrane of autophagosome gets degraded, while the rest is recycled a partial decrease in green florescence is observed among cells treated with 1 μM Sal and 0.25 μM rapamycin (positive control). However, 30 μM Sal, similar to 50 μM Cq, shows increased accumulation (shift to the right in relevant histograms; Fig. 2A, upper panel). This shows that salinomycin at higher concentrations inhibits autophagic flux, while at lower concentrations, it is an inducer of functional autophagy. Green florescence even though showed partial increase in the presence of both salinomycin and Cq, it did not show a ratiometric increase.

Next, we quantified the amount of GFP-LC3 localized to the autophagosome membrane. To do that, we removed free, cytoplasmic GFP-LC3 by permeabilization, thus we were able to directly quantify the autophagosome florescence [12]. As shown in Fig. 2A (lower panel), cells permeabilized with 0.05% saponin after treatment with either inhibitor of autophagy or inducers, showed an increase of green florescence similar to the observation made using Western blotting. As expected, salinomycin (1 μM and 30 μM), rapamycin (1 μM) and Cq (50 μM) caused the increase of green florescence due to a rise in autophagosome quantity. Similar to Western blotting results, 1 μM Sal in the presence of Cq showed a ratiometric increase in green florescence compared to 1 μM Sal or Cq alone; however, 30 μM Sal did not show such increase. This data indicates that salinomycin at higher concentrations does inhibit autophagic flux. Similarly, flow cytometric quantification of green and red fluorescence among cells expressing mTandem GFP-RFP LC3 showed lower green and red florescence in the presence of autophagic inducers (1 μM Sal, 1 μM rapamycin, and starvation), while chloroquine and 30 μM Sal showed a decrease in both green and red florescence in both MEF and PC3 cells (Fig. 3AB).

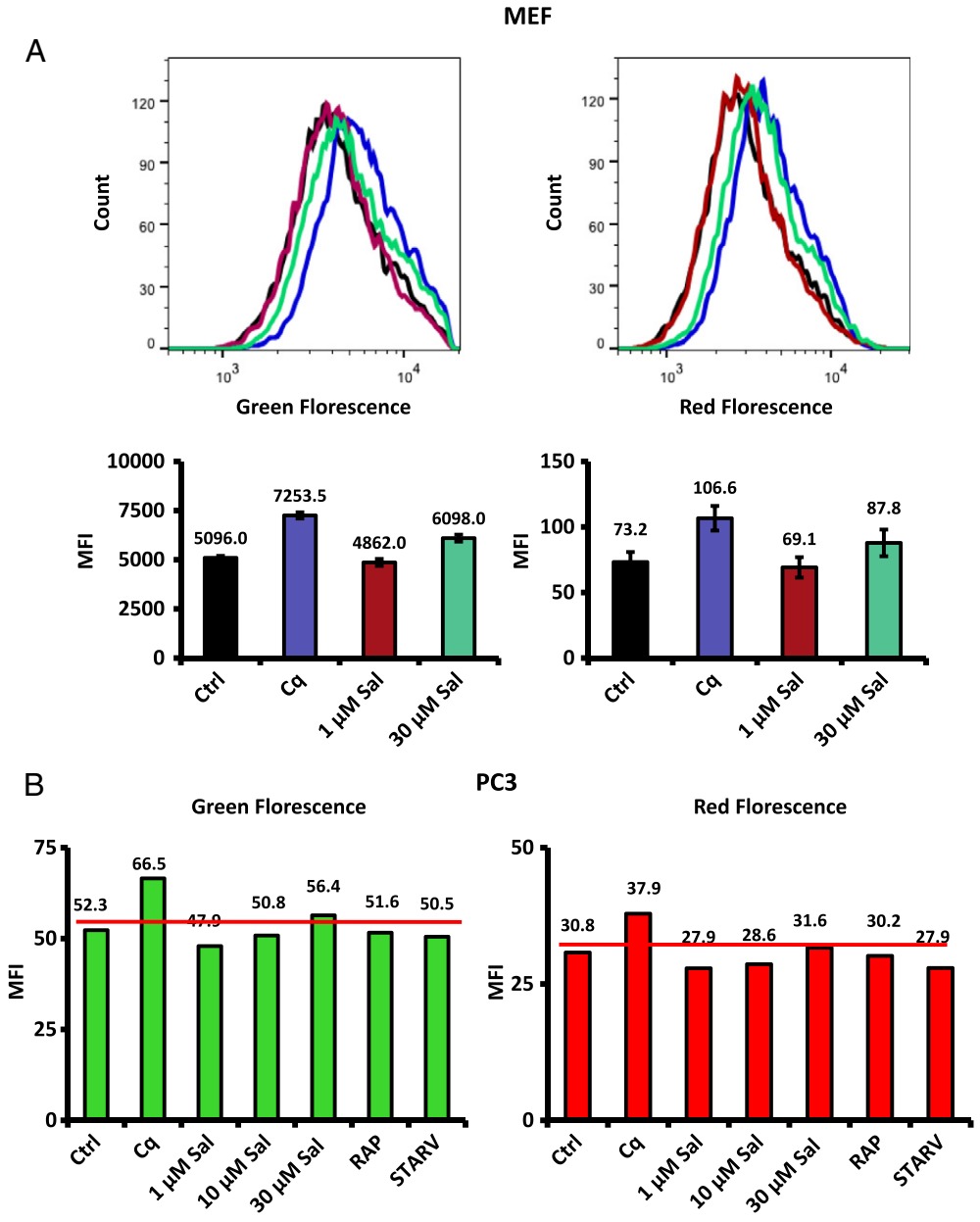

Fig. 3. The dose of salinomycin that inhibits autophagic flux depends on cell type. MEF Cells overexpressing mTandem-RPF-GFP-LC3 treated with 1 μM Sal for 6 h show decreased green florescence better than the red florescence while 30 μM Sal and chloroquine show an increase in green and red florescence compared to control cells (A). Similarly, PC3 cells also show the same pattern as MEF cells but even at 10 μM Sal shows active autophagic flux with decreased green and red florescence compared to control as rapamycin and starvation conditions (B). $N = 3$.

2.3. Live cell monitoring of autophagy

Additionally, we monitored autophagic processes using live cell imaging of GFP-LC3 expressing cells stained with Lysotracker red after treatment with 1 μM Sal for 30 min. As shown in the Fig. 4A, lysosomes are co-localized with autophagosomes by the 10th frame (100 s) and a progressive degradation of green florescence is observed with time along with final decrease in lysosome count. We further quantified total number of green punctae and lysosomes per time point, and observed an increase in the number of lysosomes and green punctae together with very synchronous fluctuations in the number of lysosomes and autophagosomes (Fig. 4B,C). Thus, effectively showing that salinomycin induces active autophagy that functions to degrade cellular organelles and proteins to counteract the cellular stress.

3. Discussion

The discovery of salinomycin's cancer stem cell targeting ability, in 2009, lead to intensive studies of its molecular mechanism of action [5]. We, and others, have studied the autophagy triggered by salinomycin [6,8,9]. Even though salinomycin is well-known to induce autophagy that functions as a cell-protective mechanism, the underlying mechanism is not fully understood, with some conflicting reports recently published. For example, Yue and colleagues, in their elaborate study using MCF7 and HMLER cancer stem cells, show that salinomycin acts as an inhibitor of autophagic flux [9]. On the contrary, in our experimental system involving PC3 (prostate cancer cells), SKBR3 (breast cancer cells) and primary human dermal fibroblast cells, as well as cells used in the original paper by Li et al., we observed an active autophagic flux in salinomycin-treated cells [6,8].

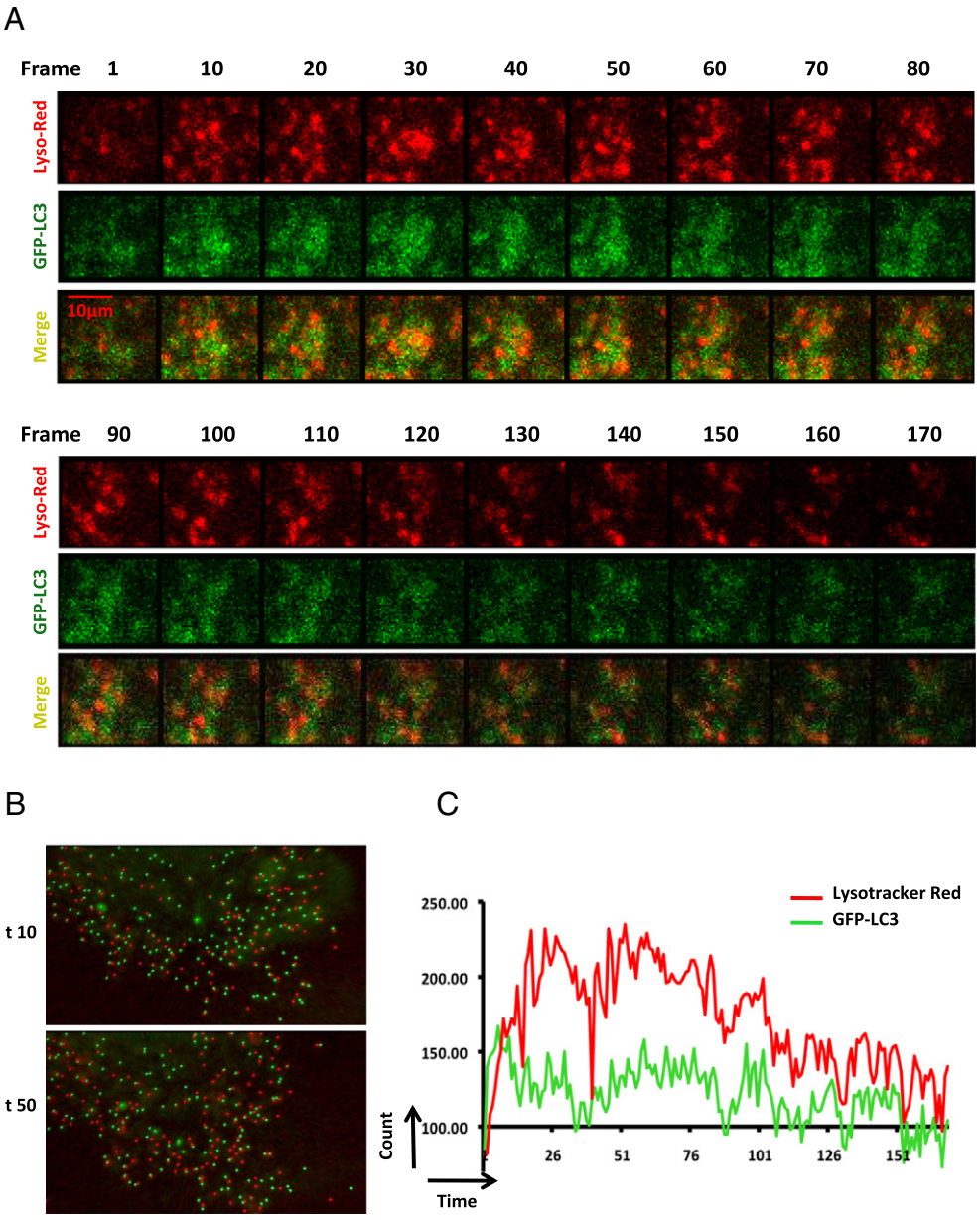

Fig. 4. Co-localization of autophagosomes and lysosomes upon salinomycin treatment. GFP-LC3 overexpressing MEF cells stained with lysotracker dye for 30 min and treated with 0.1 μM Sal were imaged using time-lapse live cell microscopy with 10 s interval for 1 h. Red-stained lysosomes co-localize with the GFP-LC3 autophagosomes (frame 30) and an eventual degradation of green and red florescence is observed from frame 100 (A). Using Bitplane Imaris software to analyze 3D images obtained with time-lapse studied lysosomal and autophagosomal count is estimated for each time frame. Frame 50 shows an increase in lysosomal (red) count and their co-localization with green autophagic punctae compared to frame 10 (B). Graphical representation of lysosomal and autophagosomal count over the period of time among salinomycin-treated cells show a similar trend in fluctuations with an increase in autophagosomal count followed by increased lysosomal count and eventual degradation (C). $N = 3$.

To understand these contradictory observations, in this study, we further examined in detail salinomycin's role in autophagic flux, using both normal murine embryonic fibroblasts and prostate cancer PC3 cells. Utilizing the densitometric analysis of LC3II expression in the presence of salinomycin and/or with autophagic inhibitors (chloroquine or bafilomycin), our study, as well as those conducted by Li and colleagues, shows a ratiometric increase at lower concentrations as compared to individual treatments. However, only a partial increase of LC3II was observed among cells treated with higher concentrations of salinomycin (Fig. 1A and Supplementary Fig. 1). Furthermore, in this study, the observation that 25 μM concentration of chloroquine treatment was only partially able to inhibit LC3II turnover triggered by salinomycin at higher concentration (10 μM). A concentration of 50 μM chloroquine shows a rise in LC3II accumulation and displays the importance of effectively blocking autophagy activity depending on the extent of the autophagy trigger. Previous studies also show that LC3II punctae are increased and co-localize with lysosomes that remain acidic upon salinomycin treatment [6,9]. However, Yue et al. further show that salinomycin inhibits lysosomal proteases thus triggering the inhibition of autophagic flux [9].

Because of the limitations of microscopy in analyzing minor fluctuations, we used flow cytometric quantification of florescence. As presented in Fig. 2 and Supplementary Fig. 3, GFP-LC3 expressing MEF and PC3, respectively, treatment with 1 μM salinomycin showed a similar trend as positive control rapamycin in decreasing green florescence intensity (increased autophagy). However, 30 μM salinomycin shows an increase of the green florescence (decrease of autophagy) as autophagy inhibitor chloroquine. Similar observations were made with mTandem GFP-RFP LC3 with both green and red florescence (Fig. 3A,B). However, PC3 cells show decreased green and red florescence even at 10 μM concentration (Fig. 3B). This demonstrates that salinomycin-mediated inhibition of autophagic flux is dependent on cell type and dosage.

While conducting studies involving GFP-LC3 overexpression in various cell lines, we observed that very high expression levels of the GFP-LC3 (induction with more than 100 MOI of adenovirus), a strong increase of the green fluorescence signal could be observed regardless of whether an activator or an inhibitor of autophagy was applied. Therefore, it is important to achieve a moderate and equal expression of the LC3-conjugated florescence proteins in cellular models cells used for the assessment of the autophagic flux.

Our time-lapse, live cell imaging further support our observations on salinomycin-triggered autophagy in the context of an active lysosomal function. Salinomycin causes severe vacuolization in the cytoplasm, as observed in our time-lapse video (Supplementary Fig. 4). The initial membrane for autophagic vessel formation also originated from sources such as Golgi, endoplasmic reticulum, etc. [13]. Thus, to study autophagic flux, we preferred to use GFP-LC3 and mTandem GFP-RFP LC3 rather than using Cyto-ID, which depends on membrane composition of the vacuoles [14]. Some studies demonstrate that vacuolization acts as an impediment for the completion of autophagic processes through disruption of lysosomal fusion with autophagosomes [15]. However, since both our studies show no such disruption in the fusion of lysosomes with the autophagosomes upon salinomycin treatment, and moreover, that the ability of ionophores to induce vacuolization is cell type dependent, one cannot exclude that excessive vacuolization at higher concentrations of salinomycin could play a secondary role in the inhibition of autophagic flux [14].

In conclusion, although autophagy is activated as a component of an initial stress response (cell coping mechanism), under the conditions of extreme stress that may cause cell death, autophagy could fail to provide protection, and also act as an enhancer of apoptosis. Several of the otherwise autophagy-promoting factors like Ambra1, Atg4d and ATG5, are differentially regulated upon cell death trigger [16–18]. Ambra1, which is mainly responsible for the initiation of autophagy, is downregulated once the cell is committed to cell death, thus inhibiting autophagy [16]. On the other hand, Atg4d during cell death is localized to the mitochondrial membrane while ATG5 nuclear localization triggers mitotic catastrophe [17,18]. Similarly, 10 μM salinomycin treatment of MCF7 cells for 16 h downregulates Beclin1 and ATG12, which are involved in the initiation and elongation of autophagy, while showing an increase at initial time points (2–8 h) and lower doses [19]. This observation further supports the dual nature of autophagic response to salinomycin treatment. Taken together, our observations suggest that the inhibition of autophagic flux by salinomycin is a secondary phenomenon.

4. Materials and Methods

4.1. Cells and Cell culture

PC3 (human prostate cancer cell line), SKBR3 (human breast cancer cell lines) and murine embryonic fibroblast (MEF) cells were cultured in complete media (RPMI or DMEM media supplemented with 10% FBS and 1% penicillin-streptomycin antibiotics) and maintained at subconfluent conditions as mentioned in our previous publication [6].

4.2. Materials and reagents

Salinomycin, rapamycin, Chloroquine and saponin, were obtained from Sigma-Aldrich and dissolved in their respective buffers as per required concentrations. Rabbit-anti-LC3b, murine anti-actin was also from Sigma-Aldrich whereas rabbit-anti-p62/SQSTRM1 was obtained from Cellular Signalling Inc. Secondary antibodies such as anti-rabbit HRP-conjugate and anti-murine HRP-conjugates were obtained from Sigma-Aldrich. Adenovirus expressing GFP-LC3 and mTandem GFP-RFP-LC3 were a kind gift from Dr. Junichi Sadoshima (Cell Biology and Molecular Medicine Rutgers University, New Jersey Medical School, USA).

4.3. Western blot

Cells cultured and treated as per experimental needs were lysed using 100 μl of lysis buffer (RIPA buffer with protease inhibitors (Complete Roche)) and mechanically sheared using 27 G ¾ inch needle and syringe. The lysate was then centrifuged at 10,000 RPM to pellet the cell debris and supernatant was collected. Protein concentration was determined using Bradford assay and equal amounts of protein samples were loaded onto the 15% PAGE gel and further proceeded as described previously [6]. The membrane was developed using Amersham ECL plus Western blot developing kit (GE technologies).

4.4. Live cell imaging and confocal microscopy

Cells plated were infected with adenovirus expressing GFP-LC3 at a viral titer of 50 MOI for 24 h and treated with lysotracker (100 nM) for 30 min were treated with various concentrations of salinomycin (0.1 μM to 1 μM) as mentioned accordingly and images were acquired using Leica DMI6000 Florescence microscope equipped with a DFC365 monochrome camera and 63× oil objective (NA 0.6–1.4) for 1 h at a rate of 10 s interval per frame and 8 *z*-stack slices of the cell is taken after setting the lower and upper limit of the *Z* section defining the cell size. The images were further analyzed using ImageJ and Bitplane Imaris software. For confocal imaging, cells pre-incubated with adenovirus expressing GFP-LC3 or mTandem GFP-RFP-LC3 at 50 MOI and treated as mentioned above were washed with PBS and fixed using 4% paraformaldehyde for 20 min at 4 °C and mounted onto a slide with mounting medium containing DAPI. Images were taken using laser scanning confocal microscope (Zeiss).

4.5. Autophagic flux analysis using flow cytometry

A total of 100,000 cells/well, plated in 6-well plates were cultured for 24 h and infected with GFP-LC3 or mTandem-GFP-RFP-LC3 for 24

or 48 h. Cells were then treated as described in the Results section, to monitor autophagy and autophagic flux, for 6 h. The cells were then washed with PBS, trypsinized and collected into an eppendorf tube. Then, the cells were centrifuged and single cell suspensions were made with 500 μl of PBS before being analyzed using Gallios Flow Cytometer (GFP with FL1 and RFP with FL4 filters both excited using 488 laser). FlowJo software was used for analysis and representation of histograms. The GFP-LC3 expressing cells are optionally incubated with 0.05% of saponin for 10 min for the respective studies.

4.6. Statistics

All statistics (one-way ANOVA) were conducted using Prism (version 6.0b) and SPSS (IBM version 20) software. A p-value of less than 0.05 was considered statistically significant unless mentioned otherwise. All the experiments were conducted as a minimum of three independent replicates unless otherwise mentioned.

Acknowledgements

We kindly thank Dr. Thommie Karlsson (application specialist at Leica Microsystems) and Dr. Venkata Ramana Rao Parasa for helping in the analysis of live cell imaging and using Bitplane Imaris software, respectively. MJL kindly acknowledges the core/startup support from Linkoping University, from Integrative Regenerative Medicine Center (IGEN), from Cancerfonden (2013/391), and from VR-NanoVision (K2012-99X-22325-01-5).

Appendix A. Supplementary data

Supplementary data to this article can be found online at http://dx.doi.org/10.1016/j.bbamcr.2014.12.022.

References

[1] D. Hanahan, R.A. Weinberg, Hallmarks of cancer: the next generation, Cell 144 (2011) 646–674.
[2] D.J. Klionsky, F.C. Abdalla, H. Abeliovich, R.T. Abraham, A. Acevedo-Arozena, et al., Guidelines for the use and interpretation of assays for monitoring autophagy, Autophagy 8 (2012) 445–544.
[3] D. Glick, S. Barth, K.F. Macleod, Autophagy: cellular and molecular mechanisms, J. Pathol. 221 (2010) 3–12.
[4] C. Zhou, W. Zhong, J. Zhou, F. Sheng, Z. Fang, Y. Wei, Y. Chen, X. Deng, B. Xia, J. Lin, Monitoring autophagic flux by an improved tandem fluorescent-tagged LC3 (mTagRFP-mWasabi-LC3) reveals that high-dose rapamycin impairs autophagic flux in cancer cells, Autophagy 8 (2012) 1215–1226.
[5] P.B. Gupta, T.T. Onder, G. Jiang, K. Tao, C. Kuperwasser, R.A. Weinberg, E.S. Lander, Identification of selective inhibitors of cancer stem cells by high-throughput screening, Cell 138 (2009) 645–659.
[6] J.R. Jangamreddy, S. Ghavami, J. Grabarek, G. Kratz, E. Wiechec, B.A. Fredriksson, R.K. Rao Pariti, A. Cieslar-Pobuda, S. Panigrahi, M.J. Los, Salinomycin induces activation of autophagy, mitophagy and affects mitochondrial polarity: differences between primary and cancer cells, Biochim. Biophys. Acta 1833 (2013) 2057–2069.
[7] J.R. Jangamreddy, M.J. Los, Mitoptosis, a novel mitochondrial death mechanism leading predominantly to activation of autophagy, Hepat. Mon. 12 (2012) e6159.
[8] T. Li, L. Su, N. Zhong, X. Hao, D. Zhong, S. Singhal, X. Liu, Salinomycin induces cell death with autophagy through activation of endoplasmic reticulum stress in human cancer cells, Autophagy 9 (2013) 1057–1068.
[9] W. Yue, A. Hamai, G. Tonelli, C. Bauvy, V. Nicolas, H. Tharinger, P. Codogno, M. Mehrpour, Inhibition of the autophagic flux by salinomycin in breast cancer stem-like/progenitor cells interferes with their maintenance, Autophagy 9 (2013) 714–729.
[10] E. Shvets, E. Fass, Z. Elazar, Utilizing flow cytometry to monitor autophagy in living mammalian cells, Autophagy 4 (2008) 621–628.
[11] P. Hundeshagen, A. Hamacher-Brady, R. Eils, N.R. Brady, Concurrent detection of autolysosome formation and lysosomal degradation by flow cytometry in a high-content screen for inducers of autophagy, BMC Biol. 9 (2011) 38.
[12] K.E. Eng, M.D. Panas, G.B. Karlsson Hedestam, G.M. McInerney, A novel quantitative flow cytometry-based assay for autophagy, Autophagy 6 (2010) 634–641.
[13] S.A. Tooze, T. Yoshimori, The origin of the autophagosomal membrane, Nat. Cell Biol. 12 (2010) 831–835.
[14] G. Morissette, E. Moreau, C.G. R, F. Marceau, Massive cell vacuolization induced by organic amines such as procainamide, J. Pharmacol. Exp. Ther. 310 (2004) 395–406.
[15] C.L. Oeste, E. Seco, W.F. Patton, P. Boya, D. Perez-Sala, Interactions between autophagic and endo-lysosomal markers in endothelial cells, Histochem. Cell Biol. 139 (2013) 659–670.
[16] G.M. Fimia, M. Corazzari, M. Antonioli, M. Piacentini, Ambra1 at the crossroad between autophagy and cell death, Oncogene 32 (2013) 3311–3318.
[17] V.M. Betin, J.D. Lane, Atg4D at the interface between autophagy and apoptosis, Autophagy 5 (2009) 1057–1059.
[18] D. Maskey, S. Yousefi, I. Schmid, I. Zlobec, A. Perren, R. Friis, H.U. Simon, ATG5 is induced by DNA-damaging agents and promotes mitotic catastrophe independent of autophagy, Nat. Commun. 4 (2013) 2130.
[19] B. Verdoodt, M. Vogt, I. Schmitz, S.T. Liffers, A. Tannapfel, A. Mirmohammadsadegh, Salinomycin induces autophagy in colon and breast cancer cells with concomitant generation of reactive oxygen species, PLoS ONE 7 (2012) e44132.